Research Article | Vol. 26, No. 24 | 26 Nov 2018 | OPTICS EXPRESS 31264
Optics EXPRESS

Power, sensitivity, and response time optimization in TDM self-reference intensity sensor networks with ring resonators

SALVADOR VARGAS[1,*] AND CARMEN VAZQUEZ[2]

[1]*Electrical Engineering Faculty, Universidad Tecnológica de Panamá, Ave. Universidad Tecnológica, El Dorado 0819-07289, Panamá, Panama*
[2]*Department of Electronic Technology, Universidad Carlos III de Madrid, Ave. Universidad No. 30, C.P: 28911, Leganés, Madrid, Spain*
[*]*salvador.vargas@utp.ac.pa*

Abstract: In this paper, we report on design rules for optimizing the response of intensity sensors embedded in ring resonators (RR) as part of a frequency based self-referencing method. Time division multiplexing sensor networks require a time response analysis for properly addressing the self-reference sensors. The selected measurement and reference frequencies are multiples of the RR Free Spectral Range to improve signal to noise ratio and avoid RR coupling coefficient (K) tolerance influence on the measurements. A weighting function that models the trade-off between high sensitivity and fast response for defining the operation point in terms of K and ring losses is also given.

© 2018 Optical Society of America under the terms of the OSA Open Access Publishing Agreement

1. Introduction

Since the first fiber optic sensor was proposed, the fotonic sensor [1], at the early days of the fiber optic communications in 1967, this field has experienced an extraordinary growth. This is mainly due to the development of fiber optic and optoelectronics technology. Many physical magnitudes have been measured such as temperature [2], strain [3], pressure [4], rotation [5], etc. Several classifications have been done according to the type of optical signal modulation used, deriving in: intensity, interferometric, polarimetric and spectroscopic sensors [6].

In intensity intrinsic fiber optic sensors (FOS) the measuring magnitude modulates the optical intensity transmitted by the fiber. Such modulation allows the use of coherent or incoherent light sources and offers advantages like reliability, size, low cost, simplicity and integration with the transmission medium. Nevertheless, these intensity sensors have problems related to non-desired optical power fluctuations. To solve this problem, different self-referencing techniques based on time division, wavelength normalization [7], spectral splitting [8], frequency division [9–12], or using counter propagating signals [13], have been reported. The frequency based self-referencing methods (FBSM) use resonant structures of finite impulse response like Sagnac [10], Michelson, and Mach Zehnder interferometers [11], sometimes based on Bragg gratings [14], or resonant structures of infinite impulse response like ring resonators (RR) [12,15]. This last technique has also been used to increase the sensitivity, introducing a FOS inside a RR structure as reported in [15].

The bandwidth used by this kind of sensors is low. Nevertheless, a single channel FOS has a relatively high cost. The aggregation of sensors through multiplexing, making them share the source and/or the detection system [14–16], reduces the cost. Time division multiplexing (TDM) on intensity modulated FOS networks, is an option that in combination with spatial division multiplexing (SDM) [17], can be used to address different sensor heads e.g., in liquid level sensors networks [18], in redundant topologies to commutate between a principal and a secondary network in case of a failure [19], or in combined TDM and dense wavelength division multiplexing (DWDM) configurations [20].

#340194 https://doi.org/10.1364/OE.26.031264
Journal © 2018 Received 20 Jul 2018; revised 17 Oct 2018; accepted 18 Oct 2018; published 13 Nov 2018

Optics EXPRESS

In TDM sensor networks, when the sensor array and/or the required sampling rate increases, time slots assigned to each sensor decrease. Then the sensor response time becomes to be important, to be able to read the sensors measurements properly. This point takes higher relevance if the sensors are embedded in infinite impulse response (IIR) resonant structures such as RR. In this case, due to the fact that the energy stored in the RR is modulated by the losses of the transducer, a correct reading requires to reach the steady state.

On the other hand, direct detection requires that the modulated signals arrive with a good power level and low noise while keeping a good sensitivity. In general, noise due to undesired power fluctuations and even the sensor sensitivity can be improved by using self-reference techniques with FOS in resonant structures, as mentioned above. Nevertheless, in TDM self-reference intensity sensor networks based on a FOS inside a RR (FOSRR), exist a compromise between the sensor response time, insertion losses and sensitivity. Moreover, all of them depend on the same design parameters.

In this paper, we carry out the study of the FOSRR design parameters, like modulation frequency, coupling coefficient and ring losses, as part of a self-referencing intensity sensor; and find those values for achieving maximum detected power, and an optimal performance either on sensitivity, time response, or both. To achieve this we define a normalized weighting factor and use the Z transform technique, already applied to the synthesis of optical filters [21] and to the design of optical demultiplexers [22]. This allows us to work with simple transfer functions to find optimum power, sensitivity, and response time values, more easily.

2. Sensor network and sensing structure

The sensor network and the basic sensing structure are shown in Fig. 1. The self-referencing sensing structure consists of a FOSRR for implementing the FBSM, a cost effective self-referencing solution that can also increase the sensitivity [15]. The optical sensor network is a combination of TDM and SDM techniques composed by N FOSRR elements addressed by time division multiplexing signals in the optical domain through different paths. The optical source is a LED modulated at two electrical frequencies, the measurement frequency f_m and the reference frequency f_r. This signal is transmitted to the network through a single optical fiber towards an optical time division demultiplexer, which distributes the signal to each branch in a time interval given by the established time slot. After that, the signal goes through the FOSRR placed in the sensing point, the different signals coming from different points, related to different measurements, are recombined in a synchronous optical time division multiplexer, to form a high speed TDM optical signal which is sent through a single fiber to the receiver. It should be noted that to maintain the synchronism the length of the N fiber paths between the demultiplexer and multiplexer, and the N ring lengths, must be the same.

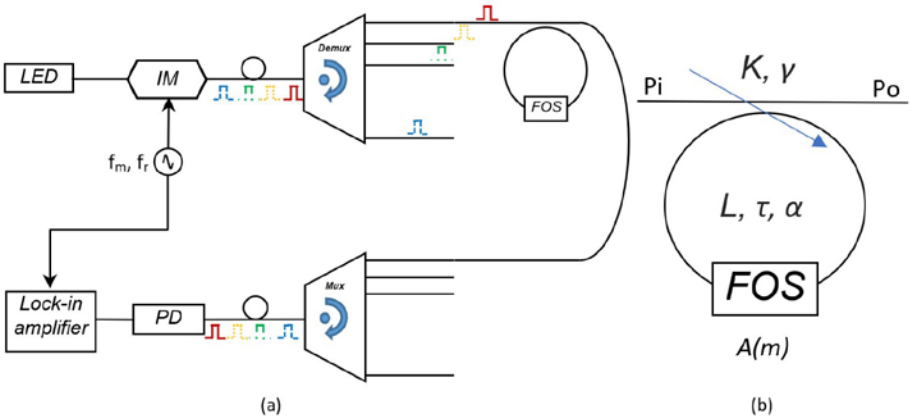

Fig. 1. (a) Sensor Network. (b) FOS in a RR (FOSRR), A is the insertion loss of FOS as function of measuring magnitude m.

Optics EXPRESS

For implementation of the network, the demux can be an optical switch that redirect the light to different fibres in different time slots, meanwhile a clock controls the commutation, as in [18]. For the mux, taking care that the time delays are equal at all the different paths, another optical switch synchronized with the input one can be used. If there is no rigid constrains in terms of bandwidth, no critical time slots are selected to accommodate slight different delay lengths with no penalty.

The interference within the RR is incoherent because the coherence time of the source, a LED, is much shorter than the time delay of the light inside the ring. The source coherence time is inversely proportional to the linewidth of the source in Hz, so this is on the order of tenths of ps, which is very unrestrictive and give us a wide range of ring lengths. For incoherent interference, there is no correlation between the phases of wave trains interfering within the ring, and they are completely random one to each other. For example, if we add wave trains, polarized along the same direction, with different amplitudes and frequencies, and random and independent phases; the expected value of the instantaneous power per unit area of the resulting waveform of this interference, taking over uniforms distribution functions between 0 and 2π, is given by:

$$E[P] = E\left[c\varepsilon_0 \left(\sum_i E_i \cos(\omega_i t + \theta_i) \right)^2 \right] = \sum_i \frac{c\varepsilon_0 E_i^2}{2} = \sum_i < P_i > \qquad (1)$$

where $E[\cdot]$ represents the statistical operator expected value, P and $<P_i>$, are the resulting instantaneous power and the average power of each wave train respectively (both per unit area). c is the speed of light in vacuum, ε_0 is the permittivity of free space. ω_i, E_i and θ_i are, the optical frequency in radians per second, the electric field amplitude and the random phase of each wave train respectively. As we can see in Eq. (1), the power we expect from this interference is the sum of the average powers of each one of the trains. The average power calculation is taken as instantaneous because the period of the train waves, at optical frequencies, is in the femtoseconds order.

In our FOSRR operating in incoherent regime, the superposition must be in power units.

2.1 Power transfer function

The Z transfer function of our IIR resonant structure, interfering in an incoherent way, relates the output and input powers, and is given by:

$$H(z) = (1-\gamma)\left[(1-K) + \frac{(1-\gamma)K^2 A e^{-\alpha L} z^{-1}}{1-(1-\gamma)(1-K)A e^{-\alpha L} z^{-1}} \right] \qquad (2)$$

where K is the power coupling coefficient, γ is the excess loss coefficient, α is the fiber attenuation in Np/Km, A is the attenuation factor introduced by the FOS and z^{-1} represents a unit delay named as τ, which is the time that light takes to travel the ring length, L.

As we can see in Eq. (2), the transfer function has two terms, the first term represents the power that passes directly from the input to the output, and the second term is the power reaching the output after passing through the ring. This second term is modulated by the losses within the ring. And before making a proper reading on this power, we should wait until the power within the RR is stabilized. In this sense the RR response time should be less than the time slot used, thus ensuring a correct reading.

2.2 Output powers

When LED power is modulated by an electrical frequency tone fe, the RR output power depends on frequency, being proportional to:

Optics EXPRESS

$$\left|H\left(e^{-j2\pi f_e\tau}\right)\right| = \frac{P_o(f_e)}{P_i(f_e)} = (1-\gamma)\left|\left[(1-K) + \frac{(1-\gamma)K^2 Ae^{-\alpha L}e^{-j2\pi f_e\tau}}{1-(1-\gamma)(1-K)Ae^{-\alpha L}e^{-j2\pi f_e\tau}}\right]\right| \quad (3)$$

where $/H(e^{-j2\pi fe\tau})/$ is the modulus of FOSRR power discrete time Fourier transform (DTFT) evaluated at any electrical frequency f_e, $/\cdot/$ represents the complex function module, P_o is the RR output power, P_i is the RR input power. Our first objective in this work is to maximize the detected power at the receiver for every FOSRR. As shown in Fig. 1, the power detected at the receiver is proportional to the input power and the overall losses, including the optical fiber attenuation, optical multiplexer and demultiplexer insertion losses and FOSRR losses. All those losses are fixed once the different components are selected, except for the FOSRR losses. Then we must work in the electrical frequencies where the resonant structure introduces the minimum losses to optimize the signal to noise ratio.

From Eq. (3), is shown that the FOSRR losses depends on K, A, γ and L values. The period or free spectral range (FSR) of the transfer function is equal to $1/\tau$.

Figure 2 shows the detected power vs the modulating frequency normalized with respect to the FSR, considering a 1 mW input power and for different values of K and A. The maximum output power of FOSRR is obtained for f_e = 0 and f_e = FSR, see Fig. 2, regardless of A and K values. This is derived from Eq. (3) and from the positive systems theory, which states that the magnitude response of a positive system can nowhere exceed its value at the origin (f_e = 0) [23]. In our case, we are using the FBSM, and the selected measurement frequency f_m is an integer multiple of the FSR to detect the maximum power level. For a silica fiber RR with 1 m of length we need to modulate at 205 MHz.

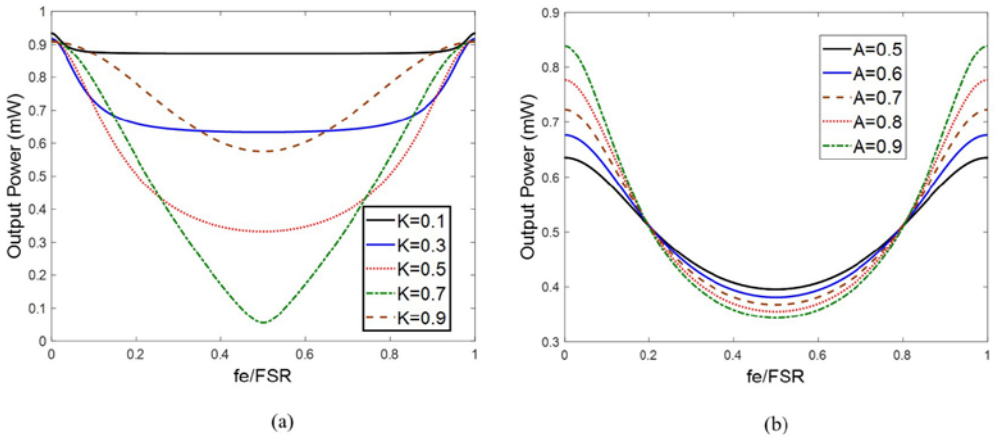

Fig. 2. FOSRR output power vs normalized frequency f/FSR for P_i = 1 mW, γ = 0.025, L = 1 Km, α = –0.046 Np/Km (a) for A = 1 and K = {0.1, 0.3, 0.5, 0.7, 0.9}, (b) for K = 0.5 and A = {0.5, 0.6, 0.7, 0.8, 0.9}.

In Fig. 2(a) is shown that the output power variations as function of K are very low, about 0.076 dB, at the normalized frequencies of 0.0135 FSR and 0.9865 FSR when A = 1, meaning a lossless sensor. In this case if the FOSRR couplers have high tolerances, and there are small A variations, any of these electrical frequencies is used as the reference frequency f_r, to minimize K tolerance influence in the different FOSRR.

In Fig. 2(b), is shown that when K = 0.5, the minimal output power variations for different A values are about 0.025 dB, at normalized frequencies given by 0.2 FSR and 0.8 FSR. Those frequencies minimize the variations in output power due to different attenuations in the FOS, being a good choice for the frequency f_r of the FBSM. The transfer function evaluated at these self-referencing frequencies is almost constant.

Optics EXPRESS

3. Sensitivity

The sensitivity is a very important parameter in any instrumentation system. It is defined as the slope of the system calibration curve. A larger sensitivity implies that the output variations are larger with slight input variations.

In our network the detected electronic signal at the reception stage for any modulation frequency f_e is given by:

$$I_{phd}\left(f_e, K, A(m)\right) = R_{phd} \cdot \left|H\left(f_e, K, A(m)\right)\right| \cdot P_{Led} \cdot L_s \tag{4}$$

where I_{phd} and R_{phd} are the photocurrent and responsivity of the photodiode, L_s are the total power losses in the light path, with exception of those given at the FOSRR represented by $H(\cdot) = P_o(\cdot)/P_i(\cdot)$, P_{Led} is the LED optical power, and m is the value of the physical magnitude to be measured by FOS.

For FBSM we define the total sensitivity S_T of a single branch as the derivative with respect to m of the ratio of I_{phd}, given in Eq. (4), evaluated at f_m over I_{phd} evaluated at f_r, and knowing that A is a function of m. This sensitivity is given by:

$$S_T = \frac{d}{dA}\left[\frac{I_{phd}\left(f_m, K, A\right)}{I_{phd}\left(f_r, K, A\right)}\right] \cdot \frac{dA}{dm} = \frac{d}{dA}\left[\frac{I_{phd}\left(f_m, K, A\right)}{I_{phd}\left(f_r, K, A\right)}\right] \cdot S_{FOS} \tag{5}$$

being the total sensitivity S_T, proportional to FOS sensitivity S_{FOS}, and to $d[I_{phd}(f_m)/I_{phd}(f_r)]/dA$. Assuming that the photodiode responsivity R_{phd}, LED emitted power P_{Led} and L_s losses are constant, the term $d[I_{phd}(f_m)/I_{phd}(f_r)]/dA$ is given by:

$$\frac{d}{dA}\left[\frac{I_{phd}\left(f_m, K, A\right)}{I_{phd}\left(f_r, K, A\right)}\right] = \frac{d}{dA}\left[\frac{\left|H\left(f_m, K, A\right)\right|}{\left|H\left(f_r, K, A\right)\right|}\right] \tag{6}$$

where $H(f_m,K,A)$ and $H(f_r,K,A)$ are the FOSRR power DTFTs, at f_m equal to an integer multiple of FSR, for example f_m = FSR, to detect the maximum power, and at f_r = 0.2 FSR to fulfill good levels of detected power independently of A variations, see Fig. 2(b).

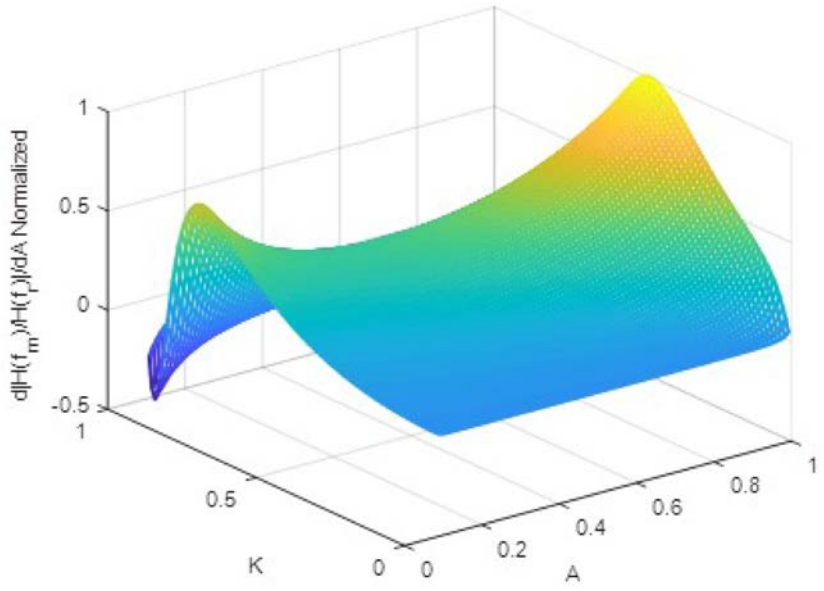

Fig. 3. 3D plot of $d[\backslash H(fm)/H(fr)\backslash]/dA$ normalized vs K (RR coupling coefficient) and A (sensor attenuation factor), with f_e = 0, γ = 0.025 and fiber attenuation inside the ring of 0.002 dB.

Optics EXPRESS

The FOS sensitivity S_{FOS} depends on the selected sensor, assuming a general solution for any sensor, the way to achieve the objective of maximizing the sensitivity is to find the operation point, i.e. the values of K and A, that maximize the term $d[|H(f_m)/H(f_r)|]/dA$.

Figure 3 shows $d[|H(f_m)/H(f_r)|]/dA$ term, normalized with respect to its maximum value, for K and A values between {0.01 – 0.99} and {0.1 – 1}, respectively. Those values avoid the cases when light passes through inside the ring only once or never (K equal to 0 or 1), and to permit an A dynamical range at least 0.1.

From Fig. 3, the maximum sensitivity occurs at a K value equal to 0.47 and A equal to 1. That is, a value close to 3 dB power coupling in the ring and a lossless FOS at the operation point. If we are only interested to have the greatest possible sensitivity, these values are the optimums and must be chose to fulfill this criterion.

4. Time-response analysis

As mentioned above the time response of each sensor element in our sensor network, is a critical parameter, especially if a TDM network is considered. If the number of sensors increases the time slot assigned for reading each one becomes shorter. Then when the sensor response time takes preponderance, we must wait until the signal that comes from each sensor is stabilized to take a correct measurement of the sensor.

The response time is determined by two components, the transit time of light signal through the entire circuit (a constant value that depends only on the total fiber length), plus the time that sensor takes to respond in a truthful manner.

In our case as FOS is inside the RR, which is an IIR system, we must wait until the stored energy within the ring reaches a stable value, to read it. To evaluate this time, we define the response time as the time it takes for the output to go from 0 to 90% of its final stable value. In FBSM there are two modulation electrical frequencies f_m and f_r, then we have two potential response times, defining as the response time the higher value between them.

The time dependent amplitude of the sensor output power, Po in Fig. 1(b) is named from now on as P_3. It is a function of the electrical modulation frequency f_e, and has two components, one that goes to the output by the coupler through path (P_{3T}), and another one coming from the ring by the coupler cross path (P_{3C}), the first and second term in Eq. (2) respectively.

In Fig. 4 is shown the time response of FOSRR at P_3, and its cross component P_{3C}, Fig. 4(a), at a measurement frequency f_m = FSR, and an input power of 1 (a. u.), N unit delays are considered.

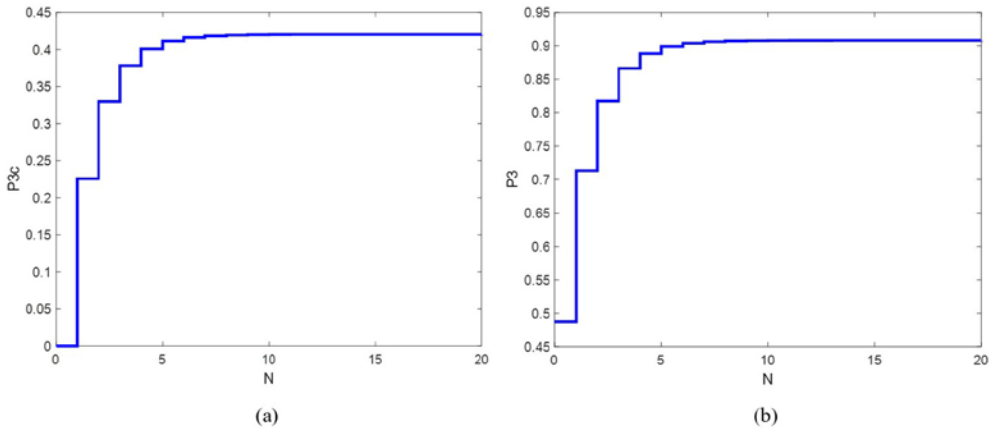

Fig. 4. FOSRR time response for f_m = FSR, and an input power of 1 (a. u.), with K = 0.5, A = 0.95, γ = 0.025 and fiber attenuation in the ring of 0.002 dB, (a) cross power component P_{3C}, (b) total power P_3.

Optics EXPRESS

In Fig. 4(a) we can see that before obtaining any power from the cross component P_{3C}, one unit delay τ, must elapses. However, in Fig. 4(b) we see that the total output at P_3, has power at the output instantly, that is at $N = 0$. Both graphs seem very similar, being the only difference that the Fig. 4(b) has a constant component added, the through component. If the coupling coefficient K is smaller, the cross component decreases, the through component increases, and the response time at P_3 can be even zero.

As we have seen the through component is instantaneous but the cross one is time dependent, so we take the response time of the cross component P_{3C} as the FOSRR response time, Tc. Also note that FOS attenuation only affects the cross component, which reinforces this definition.

The response time Tc depends on the output power after N unit delays. Expanding the second term of Eq. (2) in a sum of terms of a geometric series, evaluating at z equal to $e^{j2\pi fe/FSR}$, using the formula for the sum of N terms of a geometric series, and calculating its module. We find that the output power amplitude P_{3C}, of an electrical frequency tone f_e, for an input power of 1, after N unit delays is given by:

$$P_{3C}\left(N,f_e\right)=A\left(\left(1-\gamma\right)K\right)^2 e^{-\alpha L}\times \times\sqrt{\frac{1-2\left(A\left(1-\gamma\right)\left(1-K\right)e^{-\alpha L}\right)^N \mathrm{Cos}\left(\frac{2\pi Nf_e}{FSR}\right)+\left(A\left(1-\gamma\right)\left(1-K\right)e^{-\alpha L}\right)^{2N}}{1-2A\left(1-\gamma\right)\left(1-K\right)e^{-\alpha L}\,\mathrm{Cos}\left(\frac{2\pi f_e}{FSR}\right)+\left(A\left(1-\gamma\right)\left(1-K\right)e^{-\alpha L}\right)^2}} \quad (7)$$

the steady state value of this component is the limit as N approaches infinity, given by:

$$P_{3CS}\left(f_e\right)=\frac{A\left(\left(1-\gamma\right)K\right)^2 e^{-\alpha L}}{\sqrt{1-2A\left(1-\gamma\right)\left(1-K\right)e^{-\alpha L}\,\mathrm{Cos}\left(\frac{2\pi f_e}{FSR}\right)+\left(A\left(1-\gamma\right)\left(1-K\right)e^{-\alpha L}\right)^2}} \quad (8)$$

where P_{3CS} is the cross component steady state value at P_3 output.

Then using Eqs. (7) and (8) we solve for the number of unit delays that takes P_{3C} to reach 90% of its steady value, for both electrical modulation frequencies f_m and f_r. Finally, these results are multiplied by τ, the unit delay. For a modulation at the measurement frequency f_m = FSR, this response time can be expressed in a closed form and is given by:

$$Tc_m=\tau\cdot ceil\left[\frac{Log\left(0.1\right)}{Log\left(A\left(1-\gamma\right)\left(1-K\right)e^{-\alpha L}\right)}\right] \quad (9)$$

where Tc_m is the response time of cross power component at f_m, *ceil* means that is rounded to the next upward positive integer (including zero).

For a modulation at the reference frequency f_r = 0.2 FSR, the number of unit delays that P_{3C} takes to reach 90% of its steady value is found by numerically solving, for N, the following Eq.:

$$\sqrt{1-2\left(A\left(1-\gamma\right)\left(1-K\right)e^{-\alpha L}\right)^N Cos\left(0.4\pi N\right)+\left(A\left(1-\gamma\right)\left(1-K\right)e^{-\alpha L}\right)^{2N}}=0.9 \quad (10)$$

the numerical solution, named Ns, is rounded upward to the next integer, and is multiplied by the unit delay τ. The response time of the cross power component at reference frequency f_r, Tc_r, is given by:

$$Tc_r=\tau\cdot ceil\left(N_S\right) \quad (11)$$

Optics EXPRESS

as can be seen from Eqs. (9) and (11), both response times are proportional to the unit delay in the ring τ, and depend on the fiber ring losses, the FOS attenuation, the coupling coefficient and the excess loss factor. If we consider the excess loss factor and the fiber ring losses as fixed values, these times are a function of the coupling coefficient K, the FOS attenuation A and the unit delay τ. This delay depends on the ring length, but we can normalize the response times Tc_m and Tc_r respect to τ and find their optimal values regardless of the ring length. From now on, Tc, Tc_m, and Tc_r represent the normalized response times.

The FOSRR normalized response time Tc, is given by:

$$Tc = \max\left\{Tc_m, Tc_r\right\} \tag{12}$$

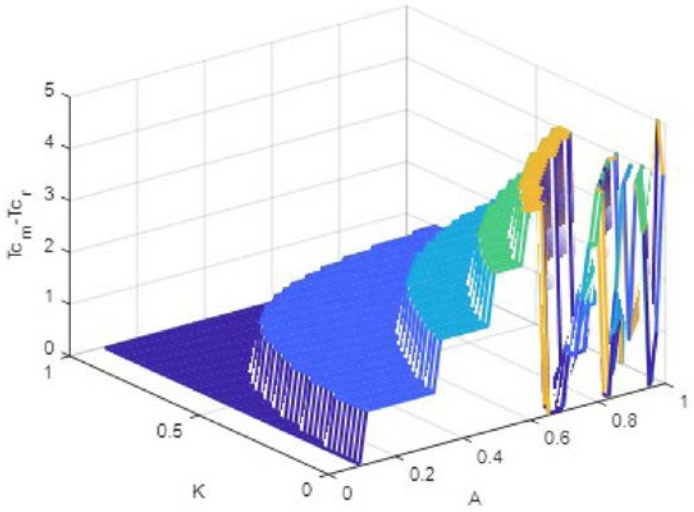

Fig. 5. 3D plot of response time difference Tc_m - Tc_r of FOSRR vs K (RR coupling coefficient) and A (sensor attenuation factor), with f_e = 0, γ = 0.025 and fiber attenuation in the ring of 0.002 dB.

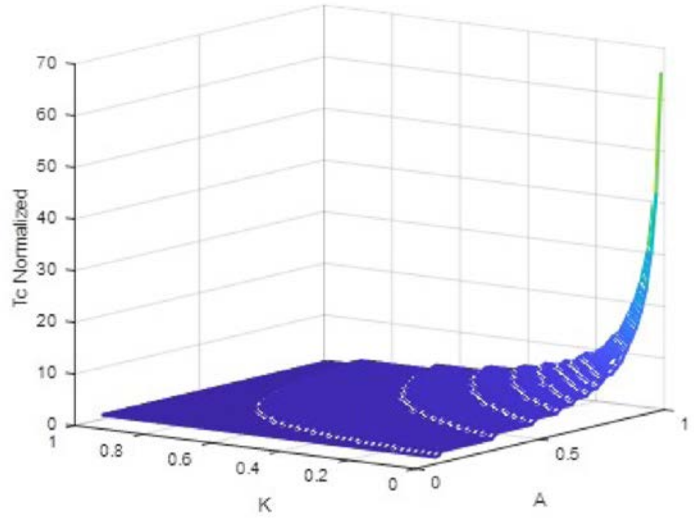

Fig. 6. 3D plot of normalized rise time of cross component in FOSRR output Tc vs K (RR coupling coefficient) and A (sensor attenuation factor), with f_e = 0, γ = 0.025 and fiber attenuation inside the ring of 0.002 dB.

Optics EXPRESS

From Eq. (9) and the numerical solving of Eq. (10), we find that the response time Tc_m is ever equal or greater than the response time Tc_r. This can be seen in Fig. 5, where a 3D plot of the response time difference between Tc_m and Tc_r as function of K and A, is shown.

As we can see in Fig. 5, never the Tc_r is greater than Tc_m. The rapid variation of the difference between them around the corner $A = 1$ and $K = 0$ in the A vs K plane, is due to in this zone there are multiple numerical solutions of Eq. (10), but only the largest one is chosen. Then, the response time Tc of the FOSRR, is considered as the response time of the cross component at measurement frequency f_m = FSR, or Tc_m, see Eq. (12).

Figure 6 shows the normalized response time of FOSRR output cross component vs K and A. Larger response times are given for large A and small K values. This is because for large A (or small loss in RR) the energy stored in the ring becomes greater, and more time is needed to reach its steady state if K is small. On the other hand, the smallest response times are given for large K values and preferably small values of A.

If we compare these results with those of the sensitivity shown in Fig. 3, we observe that medium K values (near 0.5) improves the sensitivity, but it would also be desirable to have large A values. For this reason, at choosing the A and K parameters can improve the response time but decrease the sensitivity or vice versa.

5. Weighting response time and sensitivity

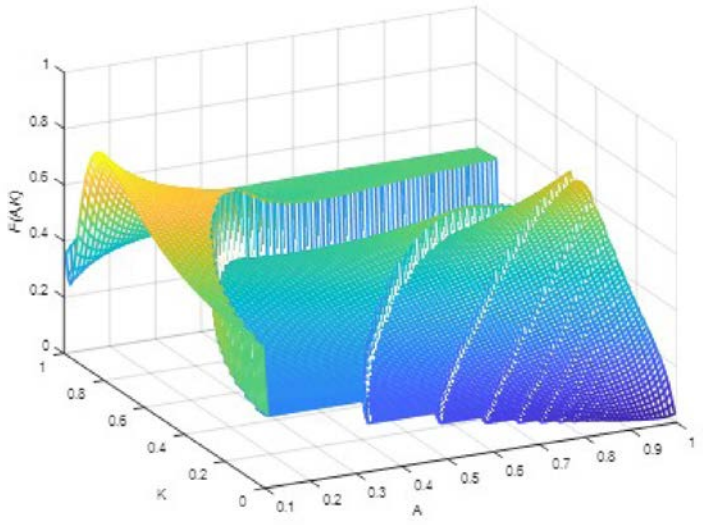

Fig. 7. 3D plot of weighting function $F(A,K)$ with x = 0.5, the same relevance for sensitivity and time response.

There are different applications for sensor networks, in some cases we have a network with few sensors or wherein the data acquisition rate can be noncritical, meanwhile in others it can be otherwise. On the other hand, the sensor sensitivity sometimes can be very important, and in other cases its value could be less relevant than time response. In a general analysis, both parameters can be considered as critical, a weighting function is defined to take both into account. This function has two terms, the normalized sensitivity weighted by a factor x, and the term related to the response time weighted by a factor of (1-x). This function is given by:

$$F(A,K) = x \times S_{Tn} + (1-x) \times \frac{1}{Tc}; \qquad x \in [0,1] \tag{13}$$

where S_{Tn} represents the normalized total sensitivity that is proportional to $d[\backslash H(f_m)/H(f_r)\backslash]/dA$ and cannot be greater than 1, Tc represents the normalized FOSRR response time and take

Optics EXPRESS

values equal or greater than 1, and x is the weighting parameter that only takes values between 0 and 1. The term $1/Tc$, can only take values less or equal to 1.

From Eq. (13), depending on the x value we can define the relevance of sensitivity and response time. As an example, if the only interest is sensitivity x is set to 1.

Figure 7 shows the weighting function from Eq. (13) with $x = 0.5$. In this case, the optimal K and A values are 0.81 and 0.1 respectively, although values of $K = 0.53$ and $A = 1$, would be a good choice too. In the same way other optimal values for K and A are found for different weightings factors, see Table 1 showing the values of K and A that are optimal for x values ranging from 0 to 1 at 0.1 increments.

From Table 1, there are three optimal operation points that should be used. When we are only interested in the response speed, the optimal values of K and A should be high, in our case they have been limited to 0.99 and 1 respectively. In this case, the FOS attenuation at operation point must be null and the coupling factor the highest the better. When we are interested in both parameters, but speed response is more relevant than sensitivity, we must use K and A values of 0.81 and 0.1 respectively. It is a FOS attenuation at the operation point of 10 dB. When the sensitivity is the relevant parameter; in this case K and A must be 0.47 and 1 respectively. Again, the attenuation at the FOS must be null.

Table 1. Optimal and alternative good values of *A* and *K* for different weighting factors *x*

Weight	*Optimal Values*		*Good Values*	
factor x	*A*	*K*	*A*	*K*
0.0	any	1	0.1	any
0.1	0.1	0.81	0.27	0.64
0.2	0.1	0.81	0.26	0.65
0.3	0.1	0.81	0.29	0.65
0.4	0.1	0.81	0.29	0.65
0.5	0.1	0.81	1	0.53
0.6	0.1	0.81	1	0.47
0.7	1	0.47	0.1	0.81
0.8	1	0.47	0.1	0.81
0.9	1	0.47	0.1	0.81
1.0	1	0.47	0.1	0.81

There are other alternatives for the parameters K and A named Good Values in Table 1. They are mainly local maxima of the weighting function.

In the case of TDM and WDM networks, the analysis in terms of time response and sensitivity is also valid. But in this case, if the different sensors are addressed by different wavelengths, additional elements such as fibre Bragg gratings should be used to extract the information of each sensor. And frequency self-reference techniques can still be applied as in [14,15] and [24].

6. Conclusions

The analysis of the transfer function of self-reference intensity sensors embedded in ring resonators, FOSRR, working in incoherent regime, and integrated on a TDM sensor network shows that there are optimum design parameters in terms of modulation frequencies, and ring resonator coupling coefficient and losses. An electrical modulating frequency of the reference signal of 0.2 FSR provides FOSRR response independent to sensor amplitude variations. The electrical modulating frequency of the measuring signal of an integer multiple of the FSR provides higher output powers improving the signal to noise ratio. There are also a pair of frequencies of 0.0135 FSR and of 0.9865 FSR where the output power is almost independent on tolerances of the RR coupling coefficient.

There is a trade-off between higher overall sensitivity and fast response. Both parameters depend on the values of RR coupling coefficient K and the FOS attenuation A at the point of operation. The maximum sensitivity occurs at a K value equal to 0.47 and A equal to 1. That is, a value close to 3 dB power coupling in the ring and a lossless FOS at the operation point. The time response of the reference signal is always smaller than the time response of the measuring signal. To achieve a short FOSRR time response, K and A should be high, the FOS

Optics EXPRESS

attenuation at operation point must be null and the coupling factor as highest as possible. When we are interested in both parameters, but speed response is more relevant than sensitivity, we must use K and A values of 0.81 and 0.1 respectively. Other local minima can give good values when both parameters are considered, a specific optimization function is provided.

Funding

Spanish Ministry of Economy and Competitiveness (TEC2015-63826-C3-2-R); Comunidad de Madrid (S2013/MIT-2790).

Acknowledgments

To SENACYT of Panamá for the support to one of the authors as member of Sistema Nacional de Investigación (SNI).

References

1. C. Menadier, C. Kissinger, and H. Adkins, "The fotonic sensor," Instrum. Control Syst. **40**(6), 114–120 (1967).
2. P. Prerana, R. K. Varshney, B. P. Pal, and B. Nagaraju, "High sensitivie fiber optic temperature sensor based on a side-polished single-mode fiber coupled to a tapered multimode overlay waveguide," J. Opt. Soc. Korea **14**(4), 337–341 (2010).
3. B. Gu, W. Yuan, M. H. Frosz, A. P. Zhang, S. He, and O. Bang, "Nonlinear fiber-optic strain sensor based on four-wave mixing in microstructured optical fiber," Opt. Lett. **37**(5), 794–796 (2012).
4. X. Wang, J. Xu, Y. Zhu, K. L. Cooper, and A. Wang, "All-fused-silica miniature optical fiber tip pressure sensor," Opt. Lett. **31**(7), 885–887 (2006).
5. Y. Yang, Z. Wang, and Z. Li, "Optically compensated dual-polarization interferometric fiber-optic gyroscope," Opt. Lett. **37**(14), 2841–2843 (2012).
6. J. M. López-Higuera, *Optical Sensors* (Ed. Universidad de Cantabria, 1998).
7. M. Kamiya, H. Ikeda, and S. Shinohara, "Analog data transmission through plastic optical fiber in robot with compensation of errors caused by optical fiber bending loss," IEEE Trans. Ind. Electron. **48**(5), 1034–1037 (2001).
8. S. Abad, M. López-Amo, F. M. Araújo, L. A. Ferreira, and J. L. Santos, "Fiber Bragg grating-based self-referencing technique for wavelength-multiplexed intensity sensors," Opt. Lett. **27**(4), 222–224 (2002).
9. S. Abad, G. M. Rego, F. M. Araújo, and A. S. Lage, "Wavelength multiplexing of frequency-based self-referenced fiber optic intensity sensors," Opt. Eng. **43**(3), 702–707 (2004).
10. J. M. Baptista, J. L. Santos, and A. S. Lage, "Self-referenced fibre optic intensity sensor based on a multiple beam Sagnac topology," Opt. Commun. **181**(4), 287–294 (2000).
11. J. M. Baptista, J. L. Santos, and A. S. Lage, "Mach-Zehnder and Michelson topologies for self-referencing fiber optic intensity sensors," Opt. Eng. **39**(6), 1636–1644 (2000).
12. C. Vázquez, J. Montalvo, D. S. Montero, and J. M. S. Pena, "Self-Referencing fiber-optic intensity sensors using ring resonators and fiber Bragg gratings," IEEE Photonics Technol. Lett. **18**(22), 2374–2376 (2006).
13. C. Sánchez-Pérez, A. García-Valenzuela, G. E. Sandoval-Romero, J. Villatoro, and J. Hernández-Cordero, "Technique for referencing of fiber-optic intensity-modulated sensors by use of counterpropagating signals," Opt. Lett. **29**(13), 1467–1469 (2004).
14. J. Montalvo, O. Frazão, J. L. Santos, C. Vázquez, and J. M. Baptista, "Radio-frequency self-referencing technique with enhanced sensitivity for coarse WDM fiber optic intensity sensors," J. Lightwave Technol. **27**(5), 475–482 (2009).
15. J. Montalvo, C. Vázquez, and D. S. Montero, "CWDM self-referencing sensor network based on ring resonators in reflective configuration," Opt. Express **14**(11), 4601–4610 (2006).
16. R. A. Perez-Herrera and M. Lopez-Amo, "Fiber optic sensor networks," Opt. Fiber Technol. **19**(6), 689–699 (2013).
17. J. P. Dakin, "Multiplexed and distributed optical fibre sensor systems," J. Phys. E Sci. Instrum. **20**(8), 954–967 (1987).
18. C. Vázquez, S. E. Vargas, J. I. Santos, J. M. Sánchez-Pena, and J. Montalvo, "Time Division Multiplexing Fibre-Optic Liquid Level Sensors using a Nematic 1x2 Optical Switch," in Proceedings of POF'04: 13th International Plastic Optical Fibres Conference, Prof. Yasuhiro Koike, (Nürnberg, 2004), pp. 351–356.
19. C. Vázquez, J. S. Pena, S. E. Vargas, A. L. Aranda, and I. Pérez, "Optical router for optical fiber sensor networks based on a liquid crystal cell," IEEE Sens. J. **3**(4), 513–518 (2003).
20. Z. Ren, K. Cui, J. Li, R. Zhu, Q. He, H. Wang, S. Deng, and W. Peng, "High-quality hybrid TDM/DWDM-based fiber optic sensor array with extremely low crosstalk based on wavelength-cross combination method," Opt. Express **25**(23), 28870 (2017).
21. S. Vargas and C. Vazquez, "Synthesis of optical filters using microring resonators with ultra-large FSR," Opt. Express **18**(25), 25936–25949 (2010).
22. S. Vargas and C. Vazquez, "Optical reconfigurable demultiplexer based on Bragg grating assisted ring resonators," Opt. Express **22**(16), 19156–19168 (2014).

Optics EXPRESS

23. K. P. Jackson, S. A. Newton, B. Moslehi, M. Tur, C. C. Cutler, J. W. Goodman, and H. J. Shaw, "Optical fiber delay-line signal processing," IEEE Trans. Microw. Theory Tech. **33**(3), 193–210 (1985).
24. D. S. Montero, C. Vázquez, J. M. Baptista, J. L. Santos, and J. Montalvo, "Coarse WDM networking of self-referenced fiber-optic intensity sensors with reconfigurable characteristics," Opt. Express **18**(5), 4396–4410 (2010).

163.117.139.121 {ts '2021-12-14 10:25:49'}